Journal of Structural Geology, Vol. 13, No. 2, pp. 151 to 164, 1991
Printed in Great Britain

0191-8141/91 $03.00+0.00
Pergamon Press plc

Segmentation and the coseismic behavior of Basin and Range normal faults: examples from east-central Idaho and southwestern Montana, U.S.A.

ANTHONY J. CRONE and KATHLEEN M. HALLER

U.S. Geological Survey, Denver, CO 80225, U.S.A.

(*Received* 1 *November* 1989; *accepted in revised form* 14 *May* 1990)

Abstract—The range-front normal faults of the Lost River and Lemhi Ranges, and the Beaverhead and Tendoy Mountains in east-central Idaho and southwestern Montana have well-preserved fault scarps on Quaternary deposits along much of their lengths. Fault-scarp morphology, the age of deposits displaced by the faults, and the morphology of the range fronts provide a basis for dividing the faults into segments that are typically 20–25 km long. The Lost River, Lemhi and Beaverhead fault zones are 141–151 km long, and each has six segments. The 60-km-long Red Rock fault (the range-front fault of the Tendoy Mountains) has two central segments that have been active in late Quaternary time; these two segments span the central 27 km of the fault.

We recognize four characteristics that help to identify segment boundaries: (1) major en échelon offsets or pronounced gaps in the continuity of fault scarps; (2) distinct, persistent, along-strike changes in fault-scarp morphology that indicate different ages of faulting; (3) major salients in the range front; and (4) transverse bedrock ridges where the cumulative throw is low compared to other places along the fault zone. Only features whose size is measured on the scale of kilometers are regarded as significant enough to represent a segment boundary that could inhibit or halt a propagating rupture.

The ability to identify segments of faults that are likely to behave as independent structural entities will improve seismic-hazard assessment. However, one should not assume that the barriers at segment boundaries will completely stop all propagating ruptures. The topographic expression of mountain ranges is evidence that, at times during their history, all barriers fail. Some barriers apparently create 'leaky' segment boundaries that impede propagating ruptures but do not completely prevent faulting on adjacent segments.

INTRODUCTION

Seismic-hazard assessments rely heavily on a basic understanding of the coseismic behavior of potentially seismogenic faults. For example, if we can estimate the length of surface faulting, the amount of displacement, and the thickness of the seismogenic crust, then we can apply empirical relations to estimate the magnitude of possible future earthquakes and, therefore, help define the hazards posed by future events. The concept of fault segmentation has important implications to hazard assessments because, if we can identify the parts of a seismogenic fault that will likely rupture during a single earthquake, then we can estimate the length and area of the fault that will generate seismic energy.

The concept of fault segmentation is based on observations that only part of long fault zones rupture during a large earthquake (Wallace 1970, Schwartz & Coppersmith 1984, 1986). Studies of historical earthquakes and paleoseismic investigations of major fault zones suggest that specific geologic features form barriers on fault planes that physically divide faults into segments (King & Yielding 1984, Smith & Bruhn 1984, Bruhn *et al.* 1987, Crone *et al.* 1987, Machette *et al.* 1987, 1991, Wheeler & Krystinik 1987, Barka & Kadinsky-Cade 1988, Fonseca 1988, Susong *et al.* 1990, dePolo *et al.* 1991, Stewart & Hancock 1991, Zhang *et al.* 1991). Barriers can slow or stop propagating coseismic ruptures (Aki 1979) and, in some cases, they seem to persist through multiple earthquake cycles (Wheeler 1987, 1989, Susong *et al.* 1990).

Faults can be subdivided into segments based on a variety of criteria and at a variety of scales (Schwartz 1988a, dePolo *et al.* 1991). For this discussion, we use the term *segment* to describe a section of a fault that we believe is likely to release most of the seismic energy during a large (**M** $\sim$ 7) surface-faulting earthquake. The geomorphic, geometric and geophysical data we discuss here support the presence of major physical discontinuities that have acted as barriers to propagating coseismic ruptures along the four range-front normal faults which we studied.

The 1983 Borah Peak earthquake on the Lost River fault is one of the most comprehensively documented, major normal-faulting earthquakes in the world. The coseismic behavior of this fault during the earthquake demonstrates the role of some barriers in controlling the extent of a propagating rupture. Geologic, seismologic and geodetic data from the 1983 earthquake show that the Lost River fault behaved as a segmented fault and that most of the energy from the main shock was released by failure of a section of the fault between two major barriers. Geologic evidence also indicates that those barriers may have confined the lateral extent of earlier ruptures on the fault (Crone *et al.* 1987, Susong *et al.* 1990). The behavior of the Lost River fault during the Borah Peak earthquake provides a valuable model of coseismic failure on major range-front normal faults. Thus, studies of the segmentation of the Lost River and similar nearby faults can have widespread applications to understanding the behavior of segmented normal

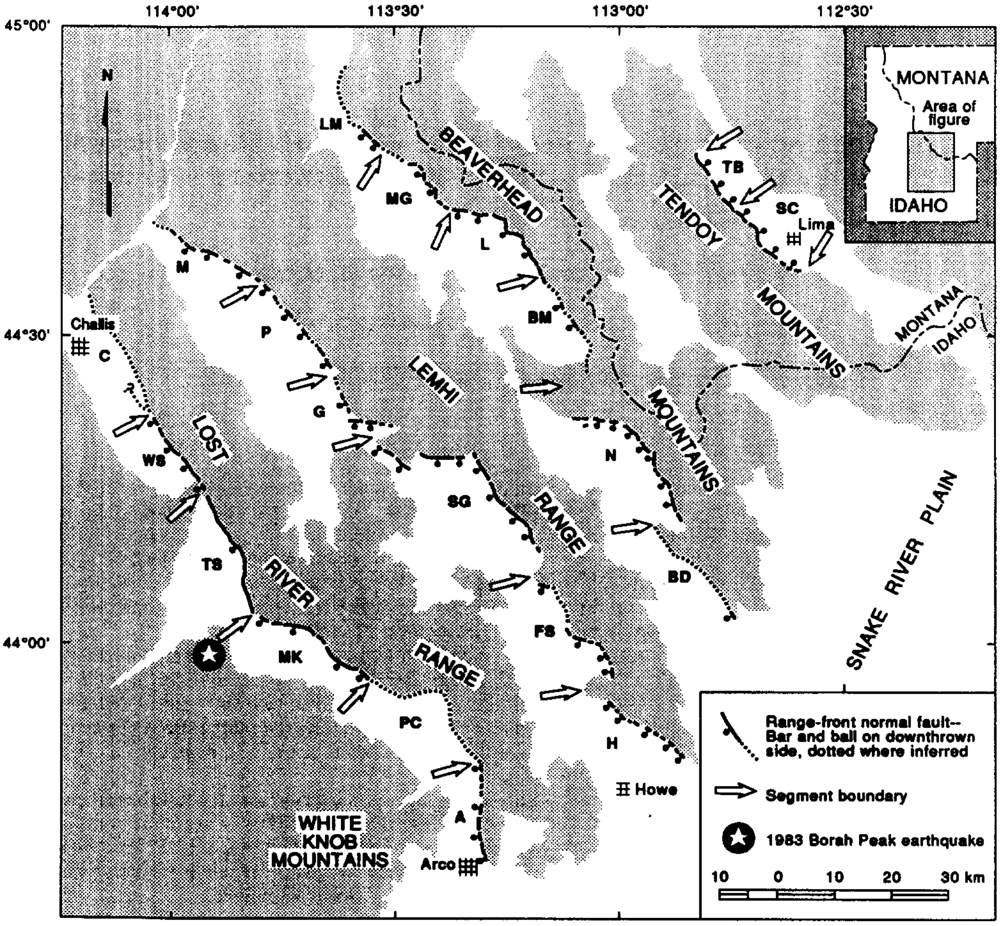

Fig. 1. Generalized map showing segments of the Lost River, Lemhi, Beaverhead and Red Rock faults in east-central Idaho and southwestern Montana. The star shows the epicenter of the 1983 Borah Peak earthquake. Shaded areas are mountainous regions. Arrows show segment boundaries. Segments are labeled as follows: *Lost River fault* (Scott *et al.* 1985, Crone *et al.* 1987)—A, Arco; PC, Pass Creek; MK, Mackay; TS, Thousand Springs; WS, Warm Spring; C, Challis; *Lemhi fault* (Haller 1988b)—H, Howe; FS, Fallert Springs; SG, Sawmill Gulch; G, Goldburg; P, Patterson; M, May; *Beaverhead fault* (Haller 1988b)—BD, Blue Dome; N, Nicholia; BM, Baldy Mountain; L, Leadore; MG, Mollie Gulch; LM, Lemhi; *Red Rock fault* (Stickney & Bartholomew 1987)—SC, Sheep Creeks; TB, Timber Butte. See Table 1 for more information about individual segments.

faults in the Basin and Range province and in other areas where the continental crust has undergone extensional deformation.

The range-front faults of the Lost River Range and adjacent mountain ranges in east-central Idaho and southwestern Montana provide an unusually good opportunity to study segmentation of normal faults because fault scarps on alluvium are well preserved and have suffered minimal cultural modification. This report summarizes the geologic evidence and characteristics used to define segments on the range-front faults of the Lost River and Lemhi Ranges, and the Beaverhead and Tendoy Mountains in Idaho and Montana (Fig. 1). We also describe some general characteristics of segment boundaries based on regional studies (Haller 1988a,b) and on detailed studies of the Lost River fault (Crone *et al.* 1987, Schwartz & Crone 1988). Our efforts to examine the segmentation of faults in a broad region have two important advantages over studying a single fault. First, the regional approach provides a more complete inventory of the kinds of features that may form segment boundaries. Secondly, this approach provides a regional perspective on the distribution of spatial and temporal patterns of surface faulting in a continental extensional tectonic setting. The faults in our study area share similarities in length, fault-plane attitude and thickness of the seismogenic layer with other major normal faults in the Basin and Range province and in other areas of normal faulting (Jackson *et al.* 1982, Schwartz 1988b, Jackson & White 1989). Thus, the characteristics of segment boundaries we describe here may be applied to faults in similar areas that are experiencing crustal extension.

SEGMENTED BEHAVIOR OF THE LOST RIVER FAULT DURING THE BORAH PEAK EARTHQUAKE

On 28 October 1983, the M_s7.3 Borah Peak earthquake ruptured part of the 141-km-long Lost River fault. The total length of surface faulting on the Lost River fault was about 36 km (Fig. 2), but geologic (Crone *et al.* 1987), seismologic (Doser & Smith 1985) and geodetic (Stein & Barrientos 1985) data show that most of the energy released by the main shock was associated with rupture of the 21-km-long Thousand Springs segment. The main shock nucleated near the base of the seismogenic crust at a depth of about 16 km (Doser & Smith 1985) at the boundary between the Thousand Springs segment and the Mackay segment to the southeast (Susong *et al.* 1990). This segment boundary coincides with a major salient at which the range front changes trend by 55° within a distance of a few kilometers. The position of the main shock with respect to this boundary indicates that the segments are separated by a geometric barrier (Aki 1979). The rupture propogated upward and unilaterally northwestward on a planar fault dipping about 45°SW (Doser & Smith 1985, Stein & Barrientos 1985) and continued along the length of the Thousand Springs segment (Crone *et al.* 1987). The largest displacement and most complex surface faulting were confined to the Thousand Springs segment (Fig. 2). On this segment, the tectonic throw reaches a maximum of 2.5-2.7 m, individual scarps are nearly 5 m high, and the zone of ground breakage is as wide as 140 m. En échelon scarps with synthetic and antithetic displacements are common.

At the northwestern end of the Thousand Springs segment, the rupture encountered a barrier where the Willow Creek Hills merge with the Lost River Range (Fig. 2). At this barrier, the rupture that nucleated at the mainshock hypocenter was either stopped or was deflected away from the Lost River fault and onto a network of smaller faults within the Willow Creek Hills. At the extreme eastern side of the hills, the 1983 scarps divide into two splays, a minor one that continues northwest about 1–2 km along the Lost River fault, and a western splay composed of discontinuous ruptures that extend across the crest and down the north flank of the Willow Creek Hills. A 4.7-km-long gap in the 1983 surface faulting is present where the Willow Creek Hills barrier merges with the Lost River fault (Fig. 2). On the Warm Spring segment northwest of this gap, the scarps are typically much less than 1 m high, and most of the surface ruptures are small discontinuous cracks. Geologic (Crone *et al.* 1987), seismologic (Boatwright 1985, Nabelek in press) and geodetic (Stein & Barrientos 1985) data all show that the Willow Creek Hills barrier effectively stopped the rupture on the range-front fault that released most of the seismic energy (Doser & Smith 1985). We believe that the scarps and cracks on the Warm Spring segment are the result of minor slip that was triggered by the severe shaking and the directivity of the rupture.

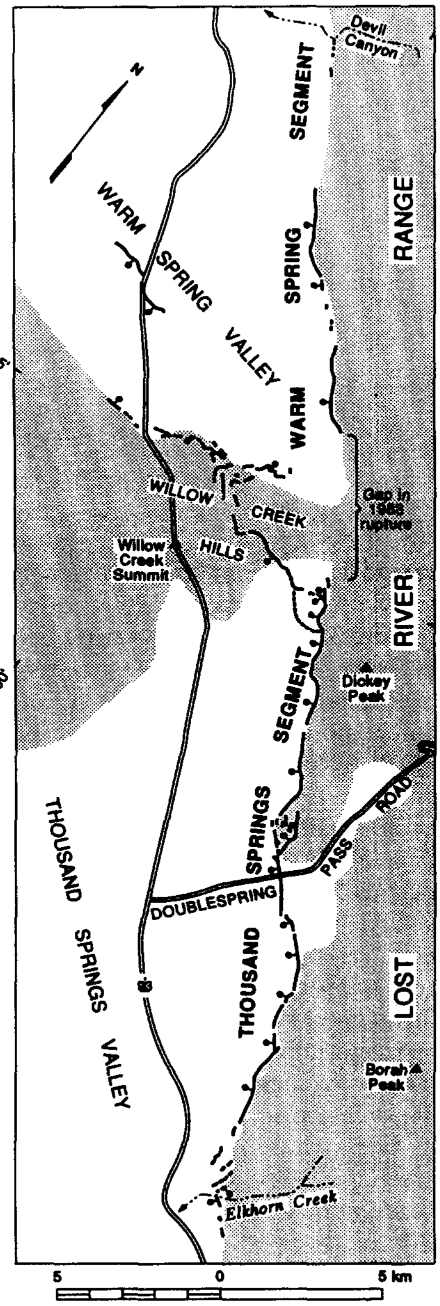

Fig. 2. Generalized map of fault scarps and ground ruptures associated with the Borah Peak, Idaho, earthquake (from Crone *et al.* 1987). Heavy lines are prominent scarps with bar and ball symbol on downthrown side; dashed lines are poorly defined scarps or cracks. Stippled areas are mountainous parts of the Lost River Range and Willow Creek Hills. The Thousand Springs segment extends from near Elkhorn Creek to the junction of the Willow Creek Hills and the Lost River Range.

SEGMENTATION OF THE RANGE-FRONT FAULTS

Prominent fault scarps on the southwest flanks of the Lost River and Lemhi Ranges, the Beaverhead Mountains, and the northeast flank of the Tendoy Mountains provide insight into the temporal and spatial distribution of late Quaternary faulting in the region. The Lost River, Lemhi and Beaverhead faults are named for their respective ranges, and the Red Rock fault bounds the northeast side of the Tendoy Mountains. On these faults, the morphology and continuity of the scarps on Quaternary deposits of similar age vary along strike; these variations provide a basis for subdividing the faults into segments. Fault-scarp morphology and the geomorphic relations between scarps and Quaternary deposits of different ages provide a simple and efficient way to broadly categorize the age of scarps, and thus identify sections of a fault that are likely to have distinctly different rupture histories.

The analysis of the morphology of Quaternary fault

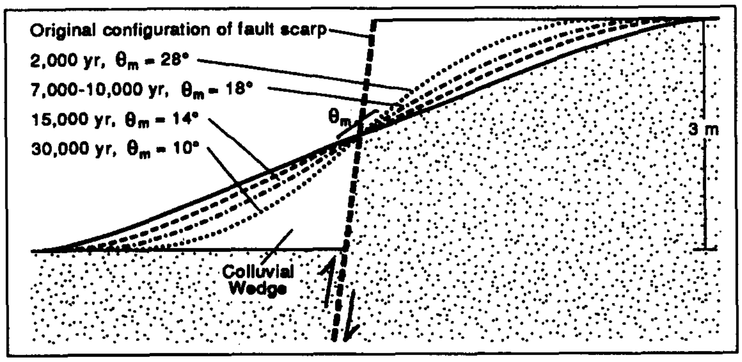

Fig. 3. Schematic diagram showing the original configuration and progressive degradation of a 3-m-high fault scarp formed on unconsolidated alluvium. The maximum slope angles (θ_m) for the 2000-, 7000–10,000- and 15,000-year-old scarps are based on empirical data for scarps of known age in the eastern Basin and Range (Bucknam & Anderson 1979); the θ_m for the 30,000-year-old scarp is computed from a mathematical regression on the empirical data. Vertical exaggeration is ×2. Arrows show direction of motion on fault. Modified after Pierce & Colman (1986).

scarps formed on unconsolidated alluvium offers an efficient means of estimating the age of prehistorical surface ruptures on single-event scarps. As soon as a fresh fault scarp forms, erosional processes begin to degrade and modify its original sharp, angular morphology into a more subdued, rounded landform (Wallace 1977). Thus, for two, single-event scarps formed in the same climate, a young scarp on alluvium has a more angular profile and a steeper slope angle on the scarp face than an equal-sized older scarp. The general age of prehistorical fault scarps can be estimated by an empirical comparison of the maximum slope angle (θ_m) and the scarp height (SH) of scarps of unknown age with scarps whose age is known (Bucknam & Anderson 1979). An alternative method estimates the age of a scarp by comparing its morphology with mathematical models of a progressively degrading scarp with time (Nash 1980, 1984, Colman & Watson 1983, Hanks *et al.* 1984, Pierce & Colman 1986, Andrews & Bucknam 1987, Hanks & Schwartz 1987, Hanks & Andrews 1989, Machette 1989). These empirical and mathematical methods show that, for 3-m-high scarps in the semi-arid eastern Basin and Range, a late Pleistocene (~30,000 years old) scarp would have θ_m of ~10°, a latest Pleistocene (~15,000 years old) scarp would have a θ_m of ~14°, an early Holocene (~7000–10,000 years old) scarp would have a θ_m of ~18°, and a late Holocene scarp (~2000 years old) would have a θ_m of ~28° (Fig. 3). Values of θ_m can vary by several degrees for equal-sized scarps of the same age because of local differences in climatic and geologic conditions. For example, Pierce & Colman (1986) show that the maximum slope angle of 3-m-high, latest Pleistocene terrace scarps near Arco, Idaho, can vary from about 14 to 20° depending on the orientation of the scarp.

The scarp height (SH) and maximum slope angle (θ_m) values cited in the following discussion are measurements of selected scarps that we provide to give the reader a general sense of the morphology of the scarps on each segment. We intentionally cite values for scarps that are approximately 3 m high to show the differences in similar-sized scarps of different ages.

We recognize that using morphologic data of multiple-event scarps to estimate the age of faulting is complicated and difficult, and that the resulting age estimates have large uncertainties (see Crone & Omdahl 1987, p. 359). Nevertheless, being fully aware of these problems and limitations, we use morphologic data of multiple-event scarps in this study to assign scarps to broad age categories, which can then be used to identify parts of the faults that have substantially different histories of surface faulting. We emphasize that, in most cases, our absolute estimates of the ages of faulting must be viewed cautiously.

Regional geologic setting

The structural style and topographic expression of the mountains and valleys in east-central Idaho and southwestern Montana are similar in many ways to other parts of the Basin and Range province (Reynolds 1979). The ranges are composed of allochthonous Precambrian and Paleozoic rocks that were thrust to the northeast starting in Cretaceous and continuing into Eocene time. Subsequent tectonism included: (a) the formation of NE-striking normal faults in Eocene time; (b) volcanism in Eocene and Oligocene time; and (c) regional uplift, additional volcanism and formation of the NW-striking normal faults that control the modern topography later in Cenozoic time. The topographic relief between the range crests and the adjacent valleys is generally about 1.5 km with maxima of about 1.9 km. The cumulative structural relief on the range-front normal faults in the region is poorly known, but locally it is probably 3–4 km (Scott *et al.* 1985) and may be as much as 6.1 km on the Lost River fault (Skipp & Hait 1977).

In the following discussion, we use the terms Pinedale-age and Bull Lake-age to describe upper Pleistocene alluvial deposits. Pinedale and Bull Lake are widely used names for the last two major episodes of glaciation in the Rocky Mountain region. The Pinedale glaciation spans a considerable amount of time in the latest Pleistocene. Some Pinedale deposits might be as much as 45,000 years old (Porter *et al.* 1983), but most are thought to be much younger. The Rocky Mountain region was extensively deglaciated by about 14,000 years ago. For this discussion, we consider Pinedale deposits to be 15,000–30,000 years old. We recognize some 'older' Pinedale deposits that we treat as being 25,000–30,000 years old and some 'younger' Pinedale deposits that we consider to be about 15,000 years old. The Bull Lake glaciation is late Pleistocene in age (commonly correlated with oxygen-isotope stage 6 of the marine record, Shackleton & Opdyke 1973). Bull Lake deposits in the Rocky Mountains are widely accepted to be about 140,000 years old (Pierce *et al.* 1976, Colman & Pierce 1981) although, in the Yellowstone National Park area, the deposits may be 135,000–160,000 years old (Pierce 1979).

The Lost River fault

Scott *et al.* (1985) divided the 141-km-long Lost River fault into six segments (Fig. 1) based on estimated age of the youngest surface faulting, the geomorphic expression of the range front, and the structural relief of the range. From northwest to southeast the segments are named the Challis, Warm Spring, Thousand Springs, Mackay, Pass Creek and Arco segments (Scott *et al.* 1985, Crone *et al.* 1987). The segments average 24 km in length with a minimum of 18 km for the Warm Spring and a maximum of 29 km for the Pass Creek segments, respectively (Table 1).

Studies of faulting on the Arco segment show that the last surface faulting occurred about 30,000 years ago (Pierce 1985). Scarps that are 3 m high have θ_m values of ~11° (Pierce 1985). Stratigraphic relations in trenches (Malde 1987) and higher scarps on progressively older Quaternary deposits show clear evidence of recurrent faulting on this segment. Repeated surface faulting has displaced 160,000 year-old deposits as much as 19 m (Pierce 1985), which yields a long-term slip rate of 0.1 mm a^{-1}.

The Pass Creek segment, the longest segment of the Lost River fault, spans a major embayment in the Lost River Range. Fault scarps on Quaternary deposits are generally absent along this segment. The oldest alluvial deposits along this part of the range front are believed to be ~15,000 years old (Pierce & Scott 1982), so surface faulting has not occurred on the Pass Creek segment within the past 15,000 years and perhaps not within the past 30,000–50,000 years (Scott *et al.* 1985).

Prominent, geomorphically young (SH = 2.2 m, θ_m = 17°) fault scarps are present along the entire length of the Mackay segment. Trenches excavated at both ends of this segment have exposed the faulted 6800 year-old Mt. Mazama volcanic ash (Scott *et al.* 1985, Schwartz & Crone 1988). In addition, a radiocarbon date on organic matter interpreted to be buried by scarp-derived colluvium suggests that the most recent faulting event occurred about 4000 years ago (Scott *et al.* 1985).

The Thousand Springs segment ruptured during the 1983 Borah Peak earthquake. The age of the surface-faulting event prior to 1983 is not well constrained, but several lines of evidence suggest that it probably occurred in middle to early Holocene time (Scott *et al.* 1985, Vincent 1985, Hanks & Schwartz 1987). Trenching studies (Schwartz & Crone 1985) and the measurement of displaced geomorphic surfaces (Vincent 1985) show that the style and amount of surface displacement from the 1983 and the pre-1983 earthquakes were similar.

The Borah Peak earthquake produced minor surface faulting on the Warm Spring segment, but this surface faulting is probably a secondary effect. Upper Pleistocene alluvial fans on this segment have pre-1983 fault scarps that are as much as 5.7 m high (Crone *et al.* 1987). Radiocarbon dates from two trenches 7.5 km apart on this segment indicate that the youngest major surface faulting occurred shortly before 5500–6200 years ago (Schwartz & Crone 1988).

The history of faulting on the Challis segment is poorly known, but reconnaissance studies have revealed little evidence of late Quaternary faulting. The range front along this segment is geomorphically subdued compared to the rest of the Lost River fault. The range front is marked by a series of low hills and the topographic relief between the range crest and the valley on

Table 1. Age of youngest movement on segments of the Lost River, Lemhi, Beaverhead and Red Rock faults, east-central Idaho and southwestern Montana

Segment name	Length (km)	Age estimate*
Lost River fault		
Arco	25	LP
Pass Creek	29	LP?
Mackay	22	MH
Thousand Springs	21	1983
Warm Spring	18	MH
Challis	25	P?
Average	24	
Beaverhead fault		
Blue Dome	25	P?
Nicholia	42	LP
Baldy Mountain	21	LP?
Leadore	23	MH
Mollie Gulch	20	LP
Lemhi	20	P?
Average	25	
Lemhi fault		
Howe	20	LP
Fallert Springs	29	LP
Sawmill Gulch	43	MH
Goldburg	12	LP
Patterson	23	MH
May	23	LP
Average	25	
Red Rock fault		
Sheep Creeks	16	MH
Timber Butte	11	LP
Average	14	

*Abbreviations for age of youngest movement are: MH, middle Holocene; LP, late Pleistocene; P, Pleistocene. Ages are queried where poorly known. Segment names are listed from southeast to northwest on individual faults.

this segment is less than 1.2 km compared to 1.5–1.8 km for other segments of the fault. The Lost River fault probably divides into two major strands (Fig. 1) on this segment. The low relief and subdued range-front morphology suggest that the Challis segment probably has the lowest slip rate of all segments on the fault.

The Lemhi fault

The Lemhi fault is 150 km long and contains at least six segments (Haller 1988b) that, from southeast to northwest, are named Howe, Fallert Springs, Sawmill Gulch, Goldburg, Patterson and May (Fig. 1 and Table 1). The segments are between 12 and 43 km long and average 25 km long (Table 1). Higher scarps on progressively older deposits show that all segments of the fault have experienced recurrent late Quaternary movement.

Data from exploratory trenches document at least five surface-faulting events on the Howe segment in the past 600,000 years; the most recent event occurred more than 15,000 years ago (Malde 1987). The scarps on the Howe segment are morphologically similar (SH = 3.4 m, θ_m = 13°) to those on the Arco segment of the Lost River fault (Haller 1988b, fig. 24), which implies that the most recent surface faulting on the Howe segment is probably late Pleistocene in age.

The most recent surface faulting on the Fallert Springs segment is also probably late Pleistocene in age because the scarps are morphologically similar to those on the Howe segment (Haller 1988b). However, for scarps of similar size, the Fallert Springs scarps have slightly steeper maximum slope angles compared to the Howe scarps, which implies that the last surface faulting on the Fallert Springs segment may be slightly younger than that on the Howe segment.

The Sawmill Gulch segment is the longest segment on the Lemhi fault (43 km) and encompasses a major embayment in the range front. Fault scarps (Haller 1988b) are present on latest Pinedale-age terraces (Pierce & Scott 1982) and have maximum slope angles (SH = 2.8–3.2 m, θ_m = 18–21°) which indicate that they are probably middle Holocene in age. Early Pinedale-age terraces have scarps that are about twice as high as the scarps on younger terraces, and therefore probably result from two faulting events. The scarps on Bull Lake-age deposits (Pierce & Scott 1982) are about three times as high as those on the early Pinedale terraces, which suggests that they could be the products of as many as six events.

The Goldburg segment, the shortest segment on the Lemhi fault (12 km), wraps around a salient in the range front. The morphology of the scarps on this segment varies considerably along strike, therefore, the boundaries of this segment may be substantially revised following further study. South of the salient, the morphology of E–W-trending, multiple-event scarps (SH = 4.2 m, θ_m = ~15°) suggests that the last surface faulting occurred about 15,000 years ago (Haller 1988b). Near the apex of the salient, these young scarps diverge from the range front and extend down the slope of the alluvial fans, whereas, an older, more degraded scarp (SH = 4.1 m, θ_m = 10°) is present at the base of the range. Apparently the most recent events on this segment did not rupture the fault strand at the base of the range. North of the salient, scarps trend NW–SE and are primarily on bedrock.

Single-event scarps are present on all Pinedale-age terraces on the Patterson segment, but their morphology (SH = 1.2–2.2 m, θ_m = 11–16°) indicates a middle Holocene age for the youngest faulting event (Haller 1988b). A trench across a single-event scarp exposed a soil that was buried by colluvium from the youngest faulting event; humus from this soil has a radiocarbon age of about 6900 years (P. L. K. Knuepfer oral communication 1989). The longer-term history of faulting on this segment is difficult to evaluate because Quaternary deposits that are old enough to have multiple-event scarps are rare along this part of the range front.

The scarps on the May segment are morphologically indistinguishable (SH = 2.9 m, θ_m = 11°) from those on the Arco segment of the Lost River fault (Haller 1988b). Therefore, like the Howe segment, we infer a late Pleistocene age for the last surface faulting and, by analogy, consider the faulting to be on the order of 30,000 years old.

The Beaverhead fault

The 151-km-long Beaverhead fault has six segments, but unlike the Lemhi fault, not all segments have scarps on deposits of late Quaternary age (Haller 1988b). From southeast to northwest, the segments are named Blue Dome, Nicholia, Baldy Mountain, Leadore, Mollie Gulch and Lemhi (Fig. 1 and Table 1). They range between 20 and 42 km long and average 25 km long (Table 1).

The history of late Quaternary faulting on the Blue Dome segment is difficult to decipher because no scarps are present on the few alluvial deposits that cross the fault. The low topographic relief and subdued morphology of the range front along the Blue Dome segment suggest that the Quaternary slip rate on this part of the fault is low relative to other parts of the fault. The amount of cumulative Quaternary throw on the strand of the fault that defines the modern range front is low because, in places, Paleozoic limestone is exposed on both sides of the fault. Our interpretation of aerial photographs suggests that the fault may divide into several strands, which may partially explain the subdued range-front morphology.

The Nicholia segment, the longest on the Beaverhead fault, coincides with a large embayment in the range front. Single- and multiple-event scarps on deposits of late Quaternary age are nearly continuous along the entire length of this segment. On the Nicholia segment, 2.2–3.7-m-high scarps on alluvium estimated to be 15,000 years old are thought to be the products of one faulting event, and 4.9–5.5-m-high scarps on alluvium estimated to be about 30,000 years old are thought to be the product of two or more events (Haller 1988b). Even though 3-m-high scarps have θ_m values (SH = 2.9–3.4 m, θ_m = 12–14°) comparable to the 15,000-year-old scarps that we have previously discussed, the entire scarp-morphology data set for this segment is similar to the data set for scarps on the Arco segment. Perhaps degradation rates are high on the Nicholia segment, which would explain why the scarps on 15,000-year-old deposits have a morphology similar to the ~30,000-year-old scarps on the Arco segment. The degraded morphology of the scarps on this segment implies that the most recent faulting probably occurred shortly after deposition of the ~15,000-year-old alluvium. At least two faulting events have occurred in the past ~30,000 years.

The absence of scarps on Quaternary alluvium on the Baldy Mountain segment is evidence that no surface faulting has occurred since the onset of the Pinedale-age episode of alluviation. However, the morphology of the mountain front shows that uplift, and thus faulting, has occurred on this segment in the late Quaternary. The junction between the range front and the piedmont is generally straight and unembayed, and major streams that emerge from the mountains have V-shaped to U-shaped cross-valley profiles along the Baldy Mountain segment. From this landform morphology, we infer that the time since uplift ceased (and thus, recurrent faulting) on this segment is no more than 100,000 years based on the criteria listed in fig. 1 of Bull (1987).

The Leadore segment, which includes a prominent embayment in the range, has generally continuous, morphologically young scarps on alluvium along its length. The most recent faulting is probably middle Holocene in age based on the morphology of single-event fault scarps (SH = 3.1 m, θ_m = 20°). The presence of higher scarps on older Pleistocene deposits provides evidence that two surface-faulting events have ruptured the Leadore segment in the past 25,000 years.

Scarps on the Mollie Gulch segment are poorly preserved and are generally located high on the colluvial slopes of the mountain front. The age of faulting is difficult to determine because there are no scarps formed on alluvium. However, we believe that the youngest surface faulting is probably late Pleistocene in age because scarps are still recognizable on steep (>25°) colluvial slopes on the range front where accelerated degradation tends to obliterate scarps relatively quickly.

The Lemhi segment is the northernmost segment of the Beaverhead fault. The youngest surface faulting on this segment predates Pinedale deposits and may be more than 100,000 years old because there are no scarps on upper Quaternary alluvium. On this segment, a series of low hills as much as 5 km wide separate the main range crest from the adjacent valley. The diffuse character of the range front implies that the Quaternary slip rate is low on this part of the fault compared to the other segments to the south.

The Red Rock fault

The Red Rock fault bounds the 60-km-long Tendoy Mountains on the northeast (Fig. 1). Quaternary deposits are not faulted along the northern 23 km or southern 10 km of this range front, so our discussion is restricted to the 27-km-long central section where Quaternary deposits are faulted. Scarps are present along the entire length of this section, but a pronounced change in their morphology is evidence that this part of the fault consists of two segments (Fig. 4), the 16-km-long Sheep Creeks segment on the southeast and the 11-km-long Timber Butte segment on the northwest (Stickney & Bartholomew 1987).

On the Sheep Creeks segment, multiple-event scarps, as much as 8 m high, are present on upper Pleistocene terraces. Higher scarps on older upper Pleistocene terraces, scarp-morphology data (Haller 1988b), and a trenching study near the southern end of the segment by Bartholomew & Stickney (1987) show evidence of two faulting events in the past 10,000–15,000 years. Radiocarbon ages from the trench date the youngest event at 3000 ± 800 years (Bartholomew 1989); we would assign a middle Holocene age to this scarp based on its morphology (SH = 2.8 m, θ_m = 20°).

The youngest scarps on the Timber Butte segment are more degraded (SH = 3.0 m, θ_m = 15°) than those on the Sheep Creeks segment (Fig. 4) and are estimated to be 10,000–15,000 years old (Haller 1988b). Multiple-event scarps are also present on this segment but we cannot estimate the age of the older event(s).

Summary of segmentation

The size, morphology and relation of fault scarps to Quaternary deposits of different ages provide a basis for subdividing the Lost River, Lemhi, Beaverhead and Red Rock faults into segments. Typically, the youngest surface faulting and the clearest evidence of recurrent latest Quarternary faulting is present on segments along the central parts of the faults. In contrast, segments near

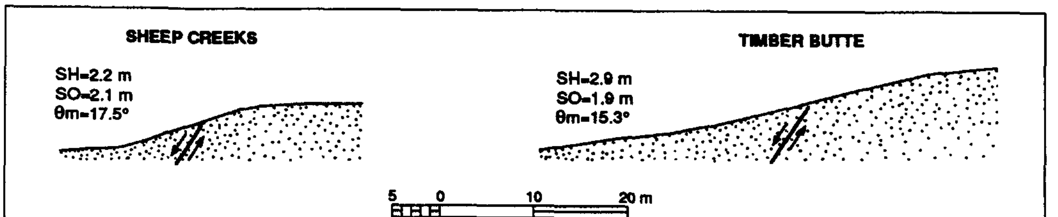

Fig. 4. Comparison of typical morphology of probable single-event scarps on the Sheep Creeks and Timber Butte segments of the Red Rock fault. SH is scarp height, SO is surface offset, and θ_m is maximum slope angle of the scarp. Horizontal and vertical scales are equal. Line with arrows shows inferred locations of faults.

the ends of faults have a subdued mountain-front morphology and, where present, very degraded fault scarps; both characteristics indicate low slip rates relative to segments along the central parts of each fault.

The segments of the Lost River, Lemhi, Beaverhead and Red Rock faults have average lengths of 24, 25, 25 and 14 km, respectively. In comparison, the segments of the Wasatch (Machette *et al.* 1987, 1991), East Cache (McCalpin 1987) and Bear Lake (Crone & Machette unpublished mapping) faults in Utah and Idaho have average lengths of about 30, 18 and 18–21 km, respectively. The Wasatch fault, Utah, which is the longest fault in the region, has unusually long segments (average 43–52 km) along its central, most active section. In contrast, the segments average 20 km in length along the distal, less active sections (Machette *et al.* 1991). The average length of segments for faults that are 100 km long or more (i.e. Lost River, Lemhi, Beaverhead and Wasatch) is 24–30 km compared to an average segment length of 14–21 km for shorter faults like the Red Rock, East Cache and Bear Lake faults. These values indicate that, if ruptures are typically confined to individual segments, most of the energy released during major normal-faulting earthquakes in the Basin and Range will result from the failure of fault surfaces that are 15–30 km long.

Many of the historical surface ruptures in Nevada are considerably longer than 30 km but individual geometric or structural segments of the faults that failed are rarely more than 30 km (dePolo *et al.* 1991, Zhang *et al.* 1991). The seismograms of these historical earthquakes show that they were composed of multiple events (Doser & Smith 1985, Jackson & White 1989) and that the maximum rupture length for an individual subevent is less than 21 km (Doser and Smith 1989). Thus geologic and seismologic data from normal-faulting earthquakes in the western United States, western Turkey (Eyidogan & Jackson 1985) and elsewhere in the world (Jackson & White 1989) indicate that individual rupture segments of major normal faults are commonly 15–30 km long.

If coseismic ruptures on major faults in the eastern Basin and Range are primarily confined to one segment and if the average segment lengths we cite are generally correct, then much of the seismic energy from large surface-faulting earthquakes in the region probably results from strain release on fault segments that are 15–30 km long. Furthermore, long faults (>100 km), such as the Lost River, Lemhi, Beaverhead and Wasatch, might generate slightly larger earthquakes than short faults (<100 km), such as the Red Rock, East Cache and Bear Lake faults, because average segment length is slightly greater.

Statistical relations between surface-rupture length and magnitude for western North America (Bonilla *et al.* 1984) imply that surface ruptures 15–30 km long are associated with earthquakes of magnitude (M_s) equal to or less than 7. However, the two largest historical earthquakes in the eastern Basin and Range province had magnitudes greater than 7, but they produced surface ruptures that were considerably shorter than the length predicted by the statistical relations. The M_s7.5 Hebgen Lake, Montana, earthquake (Doser 1985) produced about 26 km of surface rupture (see Bonilla *et al.* 1984), and the M_s7.3 Borah Peak, Idaho, earthquake produced about 36 km of surface rupture, but only about 21–25 km (Crone *et al.* 1987, Nabelek in press) of that is considered to be related to the rupture that started at the mainshock hypocenter. These two examples emphasize that the statistical relations between rupture length and magnitude should be applied cautiously, especially for faults in the eastern Basin and Range province.

IDENTIFYING SEGMENT BOUNDARIES

From our studies in Idaho and Montana, we recognize four characteristics that can help identify important segment boundaries on major, range-front normal faults: (1) prominent gaps or en échelon offsets in the continuity of fault scarps; (2) distinct, persistent changes in fault-scarp morphology along strike that likely indicate different ages of faulting; (3) major salients in the range-front; and (4) transverse bedrock ridges that indicate a local decrease in the cumulative throw on a fault. The bedrock ridges may be buried by valley fill and are expressed as gravity saddles on Bouguer gravity maps. Some features that segment faults are probably difficult to identify and, in some cases, surface faulting may extend beyond these postulated segment boundaries (dePolo *et al.* 1991). Individually, the characteristics we cite do not uniquely define a segment boundary, but we believe that the spatial coincidence of several of these characteristics is good evidence of a tectonically important segment boundary on a fault.

A scaling factor must be considered when applying these characteristics. For example, en échelon offsets or gaps of a several tens of meters or more are common within a segment. Similarly, bends or small salients are also common within a segment. However, the en échelon offsets, gaps and salients that we regard as significant indicators of segment boundaries are features whose size is measured on the scale of kilometers rather than tens of meters. Only features whose size is measured in kilometers are likely to be large enough and extend deep enough to physically interfere with a propagating rupture (Sibson 1987, 1989, Barka & Kadinsky-Cade 1989).

The characteristics of important segment boundaries that we recognize are similar to those cited in other studies of normal faults in the western United States. Transverse bedrock ridges (or transverse gravity anomalies) are present at major segment boundaries on the Wasatch fault in Utah (Wheeler & Krystinik 1987, Machette *et al.* 1991), in the Pleasant Valley–Dixie Valley–Fairview Peak area of the central Nevada Seismic Belt (Fonseca 1988, Wheeler 1989, Zhang *et al.* 1991), and on the 1872 Owens Valley, California, ruptures at the Poverty Hills (dePolo *et al.* 1991). Major salients in the range front and large en échelon offsets or gaps in scarps also correspond to important segment boundaries on the Wasatch fault (Machette *et al.* 1987,

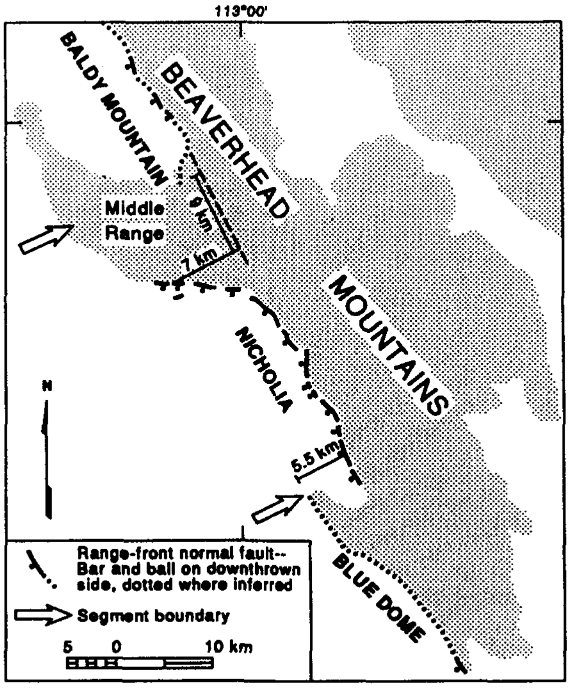

Fig. 5. Schematic map of fault scarps along part of the Beaverhead fault, east-central Idaho, showing gap between Baldy Mountain and Nicholia segments, and en échelon offset between Nicholia and Blue Dome segments. Middle Range is a transverse bedrock ridge that separates the Baldy Mountain and Nicholia segments. Fine dashed line is southeastward projection of the Baldy Mountain segment.

1991, Wheeler & Krystinik 1987) and on the Dixie Valley–Pleasant Valley, Nevada, fault system (Wallace 1984, Zhang *et al.* 1991).

En échelon offsets or gaps in scarps

Major en échelon offsets and gaps in the continuity of fault scarps are useful indicators of segment boundaries, especially where, on one side of the offset or gap, the scarps diverge from the main mountain mass (Fig. 5). Major en échelon offsets or gaps must be clearly related to tectonic causes that reflect along-strike discontinuities or geometrical irregularities in the subjacent fault. Presumably, these irregularities inhibit the propagation of a coseismic rupture (Sibson 1987, 1989). Obviously, gaps that result from surficial processes such as post-faulting erosion or deposition are meaningless in terms of the mechanical behavior and geometry of the subjacent fault.

Gaps and en échelon offsets are present at several segment boundaries on the faults we studied. On the Lost River fault, a 1.4–km-long gap in Holocene scarps and a 4.7-km-long gap in 1983 scarps separate the Warm Spring and Thousand Springs segments (Crone *et al.* 1987). Also a 3–4-km-long gap in scarps along the range front separates the Thousand Springs and Mackay segments. None of the segments on the Lost River fault are separated by en échelon offsets. On the Lemhi fault, a 2.5-km-long gap separates the Fallert Springs and Howe segments. En échelon offsets define both ends of the Goldburg segment; a 1.4-km-long offset is present at the northwestern end and a 3.8-km-long offset is present at the southeastern end. On the Beaverhead fault, a 9-km-long gap and a 7-km-wide en échelon offset separates the Baldy Mountain and Nicholia segments, and a 5.5-km-wide en échelon offset separates the Nicholia and Blue Dome segments (Fig. 5).

Persistent changes in fault-scarp morphology

We believe that fault-scarp morphology is the most useful tool for identifying fault segments because it provides insight into rupture patterns during the most recent series of surface-faulting earthquakes, and thus insight into a fault's contemporary behavior. Pronounced, persistent, along-strike changes in the morphology of fault scarps formed on alluvium are usually strong evidence that the age of surface faulting is significantly different on adjacent parts of the fault.

Several segment boundaries we studied coincide with major changes in scarp morphology. The change in the scarp morphology between the Timber Butte and Sheep Creeks segments of the Red Rock fault (Fig. 4), and the May and Patterson segments of the Lemhi fault are especially good examples.

Major salients

The Borah Peak earthquake nucleated at a segment boundary that is marked by a major salient at which the strike of the range front changes by 55° (Crone *et al.* 1987). This salient coincides with the intersection between the Lost River fault and major cross-faults in the footwall, which may have interrupted the continuity of the Lost River fault (Crone *et al.* 1987, Susong *et al.* 1990). In their study of normal faults in the Aegean region, Stewart & Hancock (1991) note that a sharp change in strike is present where footwall cross-faults intersect the main fault, and that the cross-faults probably disrupt the continuity of the main fault.

The behavior of the Lost River fault during the Borah Peak earthquake and studies of other normal faults in the western U.S. show that major range-front salients can coincide with important segment boundaries. On the Beaverhead fault, the boundary between the Leadore and Mollie Gulch segments coincides with a major salient in the range front (Fig. 1). Four major salients on the Wasatch fault coincide with persistent segment boundaries that are likely to control future coseismic ruptures (Machette *et al.* 1987, 1991, Wheeler & Krystinik 1987). Prominent changes in strike of the range front are also present at segment boundaries along the Dixie Valley–Pleasant Valley, Nevada, fault system (Zhang *et al.* 1991).

In contrast to the apparently good correlation between segment boundaries and major salients, we find an inverse correlation between segment boundaries and major embayments in our study area. Typically, major embayments are confined to a single segment. For example, the Pass Creek segment of the Lost River fault, the Sawmill Gulch segment of the Lemhi fault, and

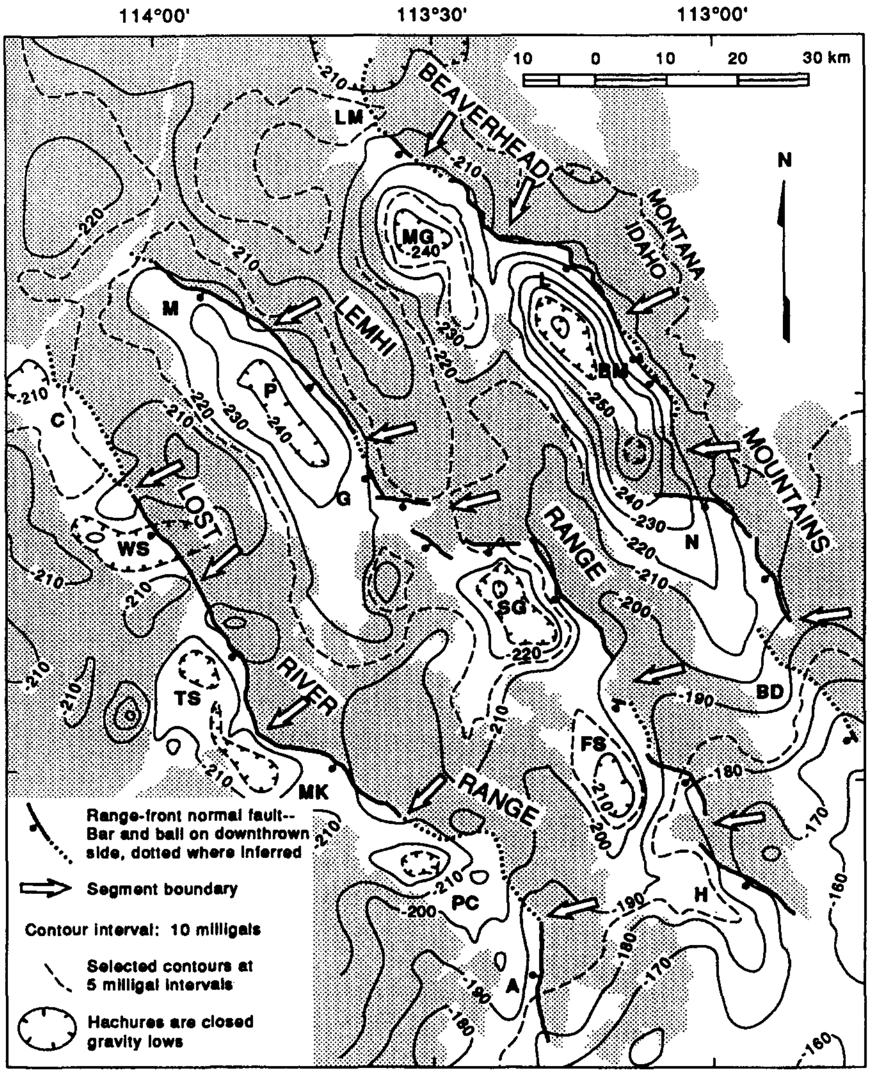

Fig. 6. Bouguer gravity anomaly map (from Bankey *et al.* 1985) and inferred segmentation of range-front faults in east-central Idaho. Arrows on rangeward side of faults show locations of segment boundaries; letters for names of segments are explained in Fig. 1. Many saddles in the gravity data coincide with inferred segment boundaries.

the Leadore and Nicholia segments of the Beaverhead fault (Fig. 1) all span major embayments in the range fronts.

Transverse bedrock ridges

Some segment boundaries are defined by transverse ridges of bedrock that are expressed either at the surface or in the subsurface. The cumulative throw on the fault at these ridges is significantly less than it is along the interior of the adjacent segments. The reduced net throw at these types of segment boundaries shows that these boundaries are long-lived features that have persisted through many earthquake cycles (Wheeler & Krystinik 1987, Wheeler 1989).

The transverse bedrock ridge that forms the barrier at the northwestern end of the Thousand Springs segment stopped the mainshock rupture of the Borah Peak earthquake. This ridge is expressed topographically as the Willow Creek Hills, a group of intra-valley hills on the southwest flank of the Lost River Range (Fig. 2). Intra-valley hills on the southwest side of both the Lemhi Range and Beaverhead Mountains presumably identify similar transverse ridges. These ridges mark the Goldburg–Sawmill Gulch segment boundary on the Lemhi fault (Fig. 1) and the Baldy Mountain–Nicholia segment boundary on the Beaverhead fault (Figs. 1 and 5).

Along some faults, transverse bedrock ridges are buried by a veneer of basin fill and have no surface expression, but geophysical data, especially gravity data, can be used to identify these buried transverse ridges (Zoback 1983). Because the cumulative throw on the fault at a transverse ridge is relatively small, the depth to bedrock in the valley at a ridge is shallow compared to the depth along the interior of a segment. Thus, the shallow bedrock of buried transverse ridges is expressed as gravity saddles on Bouguer gravity anomaly maps (Zoback 1983).

Several of our segment boundaries coincide with Bouguer gravity saddles in the adjacent valleys (Fig. 6). For many segments, especially those along the Lemhi fault, closed gravity lows coincide with the central parts of segments where throw on the fault is greatest and, thus, the basin fill is thickest. At the gravity saddles, presumably the bedrock is shallower and the basin fill is thinner. Although not all gravity saddles correlate with the segment boundaries that we have recognized from surficial geologic data, we believe that the combined analysis of Bouguer gravity data and surficial geology provide a good basis for identifying segment boundaries on range-front normal faults.

SEGMENTATION AND SEISMIC-HAZARD ASSESSMENTS

Seismic-hazard assessments can be improved by identifying the part of a fault that is likely to rupture during a single earthquake and determining the ability of individual segment boundaries to stop a propagating rupture. Segment boundaries that completely stop ruptures will allow adjacent segments to behave independently during individual earthquakes. Future studies in paleoseismology should seek to evaluate the ability of different kinds of segment boundaries to arrest ruptures (dePolo *et al.* 1991) through several seismic cycles. This evaluation is best achieved by determining the timing of successive events on adjacent segments. If the temporal pattern of surface faulting is clearly different on two adjacent segments, then the boundary between those segments has probably halted propagating ruptures repeatedly in the past and is likely to do so in the future.

This description of the behavior of segment boundaries is probably overly simplistic. The segment boundaries that we have identified in this study probably correspond to small parts of the faults (called barriers) that are consistently more resistant to rupturing and, therefore, they break less frequently (or perhaps as frequently but with less throw each time) than adjacent parts of the fault. Presumably, the past behavior of these barriers can serve as a guide to their future behavior. However, at some times during their history, all segment boundaries (barriers) must rupture, otherwise the generally continuous topographic escarpments that form mountain fronts and range crests would not exist. Thus, ultimately, no segment boundary is absolutely persistent throughout the entire history of a fault and eventually all boundaries (except those at the end of a fault) must fail.

An important complication to our description of segment-boundary behavior is that some boundaries may operate as 'leaky' boundaries. These 'leaky' boundaries can severely impede a propagating rupture, but they are not completely effective at preventing displacement on an adjacent segment. The boundary of the northwestern end of the Thousand Springs segment exhibited this type of 'leaky' behavior during the 1983 Borah Peak earthquake. At the Willow Creek Hills barrier, the mainshock rupture was stopped or was deflected away from the Lost River fault. However, enough seismic energy was transmitted through the barrier to trigger minor surface faulting on the Warm Spring segment. If more strain had accumulated on the Warm Spring segment, then the Borah Peak earthquake may have triggered a complete rupture of this segment. This type of 'leaky' behavior may well be a function of the amount of strain that has accumulated on an adjacent segment of a fault and the direction in which the rupture propagates.

We suspect that the Timber Butte–Sheep Creeks segment boundary of the Red Rock fault may have also acted as a 'leaky' boundary during the youngest faulting on the Sheep Creeks segment. Generally, the scarps on the Timber Butte segment are more degraded with more rounded crests and lower maximum slope angles than those on the Sheep Creeks segment, which implies that the Timber Butte scarps are older. However, the Timber Butte scarps that are adjacent to the segment boundary have a prominent, steep bevel, about 0.5 m high, that is superimposed on the high, degraded scarps (Haller 1988b). We interpret this bevel to reflect the youngest rupture on the Sheep Creeks segment, which extended across the segment boundary and produced minor surface rupture on the Timber Butte segment. It is important to determine if this style of behavior is typical of some segment boundaries because it has important implications for hazard assessments and for our understanding of the long-term behavior of seismogenic faults.

THE COSEISMIC BEHAVIOR OF RANGE-FRONT NORMAL FAULTS

Data from the Borah Peak earthquake and our studies of the nearby range-front faults allows us to offer some observations about the characteristics of major range-front normal faults and their probable behavior during large earthquakes. We believe that many aspects of this behavior are representative of, not only the faults we studied, but also many major normal faults in the western United States and probably in extensional terrains worldwide.

Range-front normal faults that are more than about 40 km long are probably segmented. The average length of individual segments of major normal faults in the northeastern Basin and Range is 20–25 km (Jackson & White 1989). Many major segment boundaries can be identified by using a combination of surficial and bedrock geology, and gravity data. The barriers at some segment boundaries can be very effective at limiting the lateral extent of a propagating rupture, whereas other barriers can be 'leaky' and allow secondary slip to occur on adjacent segments. Further research is needed to determine what traits of barriers make them fully, vs only partially, effective at stopping coseismic ruptures.

Precursory seismicity may not necessarily be a reliable indicator of potentially hazardous normal faults. For example, in the two decades prior to the Borah Peak earthquake, there were no earthquakes of magnitude 3.5 or greater within 25 km of the main shock (Dewey 1987). Similarly, in the 2 months before the mainshock, there were no foreshocks of magnitude 2 or greater within 50 km of the epicenter (Richins *et al.* 1987). Even though the region was generally aseismic before 1983, prominent late Pleistocene and Holocene fault scarps along all of the range-front faults are evidence that many large prehistorical earthquakes have affected the area in the past. Thus, geologic data may offer a more reliable means of identifying potentially hazardous faults than seismologic data.

Seismologic data from the Borah Peak earthquake and from other earthquakes throughout the western United States (Sibson 1982, Doser 1986) and observations of the mechanical properties of rocks (Das & Scholz 1983) show that the main shock for large earthquakes tends to nucleate at or near the base of the seismogenic layer (brittle crust). The ruptures generally propagate unilaterally away from the hypocenter and upward toward the surface along generally planar faults (Doser 1985, 1986, 1988, Doser & Smith 1985, 1989, Stein & Barrientos 1985). The unilateral propagation of a rupture implies that the earthquake must nucleate close to an unruptured barrier on the fault. Thus, recognizing major barriers on segmented normal faults may identify the most likely nucleation sites for future large earthquakes.

Estimating the magnitude of large earthquakes on normal faults can be refined by knowing the area of a fault that will likely fail during a large earthquake. By identifying major fault segments, we can delimit the probable length of a rupture. The vertical extent of a coseismic rupture will be controlled by the thickness of the seismogenic layer (Das & Scholz 1983) and, in the absence of more specific information, the attitude of a normal fault at depth can be assumed to range between 40° and 60° on the basis of seismological data from historical earthquakes (see Jackson *et al.* 1982, Doser & Smith 1989, Jackson & White 1989, Ward & Valensise 1989). The approximate area of the fault that might rupture can be computed from these parameters and used to estimate the magnitude of possible earthquakes (Wyss 1979). Magnitude estimates can be further refined by incorporating paleoseismologic data (such as displacement per event from trenching investigations) into the analysis. By knowing the rupture area and amount of displacement, one can calculate a seismic moment and moment magnitude (Hanks & Kanamori 1979) for possible earthquakes on specific segments of a fault. This approach offers an improved estimate of the size of earthquakes that a fault segment can generate compared to the more commonly used empirical approach of estimating magnitude from measurements of fault lengths or amounts of displacement (Slemmons 1977, Bonilla *et al.* 1984).

The major range-front faults in east-central Idaho and southwestern Montana offer an unusually good opportunity to study the coseismic behavior and segmentation of normal faults. Geologic, seismologic and geodetic data from the 1983 Borah Peak earthquake provide a detailed picture of the coseismic failure of a major normal fault, and, from our studies, we recognize several characteristics that can be used to identify segment boundaries of normal faults. Further studies are needed to make a more comprehensive inventory of the types and scales of features that segment normal faults. These studies will contribute to a better understanding of the processes and mechanics of fault segmentation, especially because studies of historical surface-faulting earthquakes in the Basin and Range province have shown that a variety of features can act as barriers and affect earthquake ruptures on faults (dePolo *et al.* 1991). Paleoseismic investigations are also needed to determine the regional variations in time and space of surface-faulting earthquakes. From these regional studies, we can identify patterns of temporal and spatial clustering of earthquakes, which will provide insight into the way strain accumulates and is released in the upper crust. These lines of research will contribute to a better understanding of the long-term behavior of individual faults and groups of faults in a region, which, ultimately, will improve our ability to realistically assess earthquake hazards.

Acknowledgements—We wish to thank R. E. Anderson, J. A. Jackson, S. F. Personius, D. P. Schwartz and I. S. Stewart for their thoughful comments and careful reviews of this manuscript.

REFERENCES

Aki, K. 1979. Characterization of barriers on an earthquake fault. *J. geophys. Res.* **84**, 6140–6148.

Andrews, D. J. & Bucknam, R. C. 1987. Fitting degradation of shoreline scarps to a nonlinear diffusion model. *J. geophys. Res.* **92**, 12,857–12,867.

Bankey, V., Webring, M., Mabey, D. R., Kleinkopf, M. D. & Bennett, E. H. 1985. Complete Bouguer gravity anomaly map of Idaho. *U.S. geol. Surv. Misc. Field Studies Map* **MF-1773**. Scale 1:500,000.

Barka, A. A. & Kadinsky-Cade, K. 1988. Strike-slip fault geometry in Turkey and its influence on earthquake activity. *Tectonics* **7**, 663-684.

Barka, A. A. & Kadinsky-Cade, K. 1989. Effects of restraining stepovers on earthquake rutpure. *U.S. geol. Surv. Open-file Rep.* **89-315**, 67–79.

Bartholomew, M. J. 1989. Road log No. II—The Red Rock fault and complexly deformed structures in the Tendoy and Four Eyes Canyon Thrust Sheets—Examples of late Cenozoic and late Mesozoic deformation in southwestern Montana. *Northwest Geol.* **18**, 21–35.

Bartholomew, M. J. & Stickney, M. C. 1987. Late Quaternary faulting in southwest Montana. *Geol. Soc. Am. Abs. w. Prog.* **19**, 258–259.

Boatwright, J. 1985. Characteristics of the aftershock sequence of the Borah Peak, Idaho, earthquake determined from digital recordings of the events. *Bull. seism. Soc. Am.* **75**, 1265–1284.

Bonilla, M. G., Mark, R. K. & Lienkaemper, J. J. 1984. Statistical relations among earthquake magnitude, surface rupture length, and surface fault displacement. *Bull. seism. Soc. Am.* **74**, 2379–2411.

Bruhn, R. L., Gibler, P. R. & Parry, W. T. 1987. Rupture characteristics of normal faults—An example from the Wasatch fault zone, Utah. In: *Continental Extensional Tectonics* (edited by Coward, M. P., Dewey, J. F. & Hancock, P. L.). *Spec. Publs geol. Soc. Lond.* **28**, 337–353.

Bucknam, R. C. & Anderson, R. E. 1979. Estimation of fault-scarp ages from a scarp-height–slope-angle relationship. *Geology* **7**, 11–14.

Bull, W. B. 1987. Relative rates of long-term uplift of mountain fronts. In: *Proc. Conference XXXIX—Directions in Paleoseismology* (edited by Crone, A. J. & Omdahl, E. M.). *U.S. geol. Surv. Open-file Rep.* **87-673**, 192–202.

Colman, S. M. & Pierce, K. L. 1981. Weathering rinds on andesitic and basaltic stones as a Quaternary age indicator, Western United States. *Prof. Pap. U.S. geol. Surv.* **1210**.

Colman, S. M. & Watson, K. 1983. Ages estimated from a diffusion equation model for scarp degradation. *Science* **221**, 263–265.

Crone, A. J., Machette, M. N., Bonilla, M. G., Lienkaemper, J. J., Pierce, K. L., Scott, W. E. & Bucknam, R. C. 1987. Surface faulting accompanying the Borah Peak earthquake and segmentation of the Lost River fault, central Idaho. *Bull. seism. Soc. Am.* **77**, 739–770.

Crone, A. J. & Omdahl, E. M. (editors) 1987. *Proc. Conference XXXIX—Directions in Paleoseismology. U.S. geol. Surv. Open-file Rep.* **87-673**.

Das, S. & Scholz, C. H. 1983. Why large earthquakes do not nucleate at shallow depths. *Nature* **305**, 621–623.

dePolo, C. M., Clark, D. G., Slemmons, D. B. & Ramelli, A. R. 1991. Historical surface faulting in the Basin and Range Province, western North America: implications for fault segmentation. *J. Struct. Geol.* **13**, 123–136.

Dewey, J. W. 1987. Instrumental seismicity of central Idaho. *Bull. seism. Soc. Am.* **77**, 819–836.

Doser, D. I. 1985. Source parameters and faulting processes of the 1959 Hebgen Lake, Montana, earthquake sequence. *J. geophys. Res.* **90**, 4537–4555.

Doser, D. I. 1986. Earthquake processes in the Rainbow Mountain–Fairview Peak–Dixie Valley, Nevada, region 1954–1959. *J. geophys. Res.* **91**, 12,572–12,586.

Doser, D. I. 1988. Source parameters of earthquakes in the Nevada seismic zone, 1915–1943. *J. geophys. Res.* **93**, 15,001–15,015.

Doser, D. I. & Smith, R. B. 1985. Source parameters of the 28 October 1983 Borah Peak, Idaho, earthquake from body wave analysis. *Bull. seism. Soc. Am.* **75**, 1041–1051.

Doser, D. I. & Smith, R. B. 1989. An assessment of source parameters of earthquakes in the Cordillera of the Western United States. *Bull. seism. Soc. Am.* **79**, 1383–1409.

Eyidogan, H. & Jackson, J. 1985. A seismological study of normal faulting in the Demirci, Alasehir and Gediz earthquakes of 1969–70 in western Turkey: implications for the nature and geometry of deformation in the continental crust. *Geophys. J. R. astr. Soc.* **81**, 569–607.

Fonseca, J. 1988. The Sou Hills—A barrier to faulting in the central Nevada seismic belt. *J. geophys. Res.* **93**, 475–489.

Haller, K. M. 1988a. Proposed segmentation of the Lemhi and Beaverhead faults, Idaho and Red Rock fault, Montana—Evidence from studies of fault-scarp morphology. *Geol. soc. Am. Abs. w. Prog.* **20**, 418–419.

Haller, K. M. 1988b. Segmentation of the Lemhi and Beaverhead faults, east-central Idaho, and Red Rock fault, southwest Montana, during the late Quaternary. Unpublished thesis, University of Colorado, Boulder.

Hanks, T. C. & Andrews, D. J. 1989. Effect of far-field slope on morphologic dating of scarplike landforms. *J. geophys. Res.* **94**, 565–573.

Hanks, T. C., Bucknam, R. C., Lajoie, K. R. & Wallace, R. E. 1984. Modification of wave-cut and faulting-controlled landforms. *J. geophys. Res.* **89**, 5771–5790.

Hanks, T. C. & Kanamori, H. 1979. A moment magnitude scale. *J. geophys. Res.* **84**, 2348–2350.

Hanks, T. C. & Schwartz, D. P. 1987. Morphologic dating of the pre-1983 fault scarp on the Lost River fault at Doublespring Pass road, Custer County, Idaho. *Bull. seism. Soc. Am.* **77**, 837–846.

Jackson, J. A., Gagnepain, J., Houseman, G., King, G. C. P., Papadimitriou, P., Soufleris, C. & Virieux, J. 1982. Seismicity, normal faulting, and the geomorphological development of the Gulf of Corinth (Greece): the Corinth earthquakes of February and March 1981. *Earth Planet Sci. Lett.* **57**, 377–397.

Jackson, J. A. & White, N. J. 1989. Normal faulting in the upper continental crust: observations from regions of active extension. *J. Struct. Geol.* **11**, 15–36.

King, G. & Yielding, G. 1984. The evolution of a thrust fault system—Processes of rupture initiation, propagation and termination in the 1980 El Asnam (Algeria) earthquake. *Geophys. J. R. astr. Soc.* **77**, 915–933.

Machette, M. N. 1989. Slope-morphometric dating. In: *Dating Methods Applicable to Quaternary Geologic Studies in the Western United States* (edited by Forman, S. L.). *Utah Geol. & Min. Surv. Misc. Publ.* **89-7**, 30–42.

Machette, M. N., Personius, S. F., Nelson, A. R., Schwartz, D. P. & Lund, W. R. 1991. The Wasatch fault zone, Utah—segmentation and history of the Holocene earthquakes. *J. Struct. Geol.* **13**, 137–149.

Machette, M. N., Personius, S. F. & Nelson, A. R. 1987. Quaternary geology along the Wasatch fault zone—Segmentation, recent investigation, and preliminary conclusions. In: *Assessment of Regional Earthquake Hazards and Risk along the Wasatch Front, Utah* (edited by Gori, P. L. & Hays, W. W.). *U.S. geol. Surv. Open-file Rep.* **87-585**, A1-A72.

Malde, H. E. 1987. Quaternary faulting near Arco and Howe, Idaho. *Bull. seism. Soc. Am.* **77**, 847–867.

McCalpin, J. 1987. Late Quaternary tectonics and earthquake hazard in Cache Valley, Utah. *U.S. geol. Surv. Final Tech. Rep.* (Contract 14-08-0001-G1091).

Nabelek, J. In press. Planar vs listric faulting: the rupture process and fault geometry of the 1983 Borah Peak, Idaho, earthquake from inversion of teleseismic body waves. *J. geophys. Res.*

Nash, D. B. 1980. Morphologic dating of degraded normal fault scarps. *J. Geol.* **88**, 353–360.

Nash, D. B. 1984. Morphologic dating of fluvial terrace scarps and fault scarps near West Yellowstone, Montana. *Bull. geol. Soc. Am.* **95**, 1413–1424.

Pierce, K. L. 1979. History and dynamics of glaciation in the northern Yellowstone National Park area. *Prof. Pap. U.S. geol. Surv.* **729-F**.

Pierce, K. L. 1985. Quaternary history of faulting on the Arco segment of the Lost River fault, central Idaho. In: *Proc. Workshop XXVIII on the Borah Peak, Idaho, Earthquake* (edited by Stein, R. S. & Bucknam, R. C.). *U.S. geol. Surv. Open-file Rep.* **85-290**, 195–206.

Pierce, K. L. & Colman, S. M. 1986. Effect of height and orientation (microclimate) on geomorphic degradation rates and processes, late-glacial terrace scarps in central Idaho. *Bull geol. Soc. Am.* **97**, 869–885.

Pierce, K. L., Obradovich, J. D. & Friedman, I. 1976. Obsidian hydration dating and correlation of Bull Lake and Pinedale glaciations near West Yellowstone, Montana. *Bull. geol. Soc. Am.* **87**, 703–710.

Pierce, K. L. & Scott, W. E. 1982. Pleistocene episodes of alluvial-gravel deposition, southeastern Idaho. In: *Cenozoic Geology of Idaho* (edited by Bonnichsen, B. & Breckenridge, R. M.). *Bull. Idaho Bur. Mines Geol.* **26**, 685–702.

Porter, S. C., Pierce, K. L. & Hamilton, T. D. 1983. Late Wisconsin mountain glaciation in the Western United States. In: *Late Quaternary Environments of the United States*, Vol. 1 (edited by Wright, H. E.). University of Minnesota Press, Minneapolis, Minnesota, 71–111.

Reynolds, M. W. 1979. Character and extent of Basin-Range faulting, western Montana and east-central Idaho. *Rocky Mtn Ass. Geol. & Utah Geol. Ass.* 1979 *Basin and Range Symposium*, 185–193.

Richins, W. D., Pechmann, J. C., Smith, R. B., Langer, C. J., Goter, S. K., Zollweg, J. E. & King, J. J. 1987. The 1983 Borah Peak, Idaho, earthquake and its aftershocks *Bull. seism. Soc. Am.* **77**, 694–723.

Schwartz, D. P. 1988a. Geologic characterization of seismic sources: moving into the 1990s. In: *Earthquake Engineering and Soil Dynamics II—Recent Advances in Ground Motion Evaluation* (edited by Von Thune, J. L.). *Geotech. Spec. Publs Am. Soc. Civil Engrs* **20**, 1–42.

Schwartz, D. P. 1988b. Paleoseismicity and neotectonics of the Cordillera Blanca fault zone, northern Peruvian Andes. *J. geophys. Res.* **93**, 4712–4730.

Schwartz, D. P. & Coppersmith, K. J. 1984., Fault behavior and characteristic earthquakes—Examples from the Wasatch and San Andreas fault zones. *J. geophys. Res.* **89**, 5681–5698.

Schwartz, D. P. & Coppersmith, K. J. 1986. Seismic hazards—New trends in analysis using geologic data. In: *Active Tectonics, Studies in Geophysics*. National Academy Press, Washington, DC, 215–230.

Schwartz, D. P. & Crone, A. J. 1985. The 1983 Borah Peak earthquake—A calibration event for quantifying earthquake recurrence and fault behavior on Great Basin normal faults. In: *Proc. Workshop XXVIII on the Borah Peak, Idaho, Earthquake* (edited by Stein, R. S. & Bucknam, R. C.). *U.S. geol. Surv. Open-file Rep.* **85-290**, 153–160.

Schwartz, D. P. & Crone, A. J. 1988. Plaeoseismicity of the Lost River fault zone, Idaho—Earthquake recurrence and segmentation. *Geol. Soc. Am. Abs. w. Prog.* **20**, 228.

Scott, W. E., Pierce, K. L. & Hait, H. M., Jr. 1985. Quaternary tectonic setting of the 1983 Borah Peak earthquake, central Idaho. *Bull. seism. Soc. Am.* **75**, 1053–1066.

Shackleton, N. J. & Opdyke, N. D. 1973. Oxygen isotope and palaeomagnetic stratigraphy of equatorial Pacific core V28-238: oxygen isotope temperatures and ice volumes on a 10^5 year scale. *Quat. Res.* **3**, 39–55.

Sibson, R. H. 1982. Fault zone models, heat flow, and the depth distribution of earthquakes in the continental crust of the United States. *Bull. seism. Soc. Am.* **72**, 151–163.

Sibson, R. H. 1987. Effects of fault heterogeneity on rupture propagation. In: *Proc. Conference XXXIX—Directions in Paleoseismology* (edited by Crone, A. J. & Omdahl, E. M.). *U.S. geol. Surv. Open-file Rep.* **87-673**, 362–372.

Sibson, R. H. 1989. Earthquake faulting as a structural process. *J. Struct. Geol.* **11**, 1–14.

Skipp, B. & Hait, M. H., Jr. 1977. Allochthons along the northeast margin on the Snake River Plain, Idaho. In: *Rocky Mountain Thrust Belt Geology and Resources* (edited by Heisey, E. L., Norwood, E. R., Wach, P. H. & Hall, L. A.). *Wyoming geol. Ass. 29th Ann. Field Conf. Guidebook* 499–515.

Slemmons, D. B. 1977. Faults and earthquake magnitude. *U.S. Army Corp. Engrs Waterways Exp. Sta. Misc. Pap.* **S-73-1**.

Smith, R. B. & Bruhn, R. L. 1984. Intraplate extensional tectonics of the eastern Basin-Range: inferences on structural style from seismic reflection data, regional tectonics, and thermal–mechanical models of brittle–ductile deformation. *J. geophys. Res.* **89**, 5733–5762.

Stein, R. S. & Barrientos, S. 1985. Planar high-angle faulting in the Basin and Range—Geodetic analysis of the Borah Peak, Idaho, earthquake. *J. geophys. Res.* **90**, 11,355–11,366.

Stewart, I. S. & Hancock, P. L. 1991. Scales of structural heterogeneity within neotectonic normal fault zones in the Aegean region. *J. Struct. Geol.* **13**, 191–204.

Stickney, M. C. & Bartholomew, M. J. 1987. Seismicity and late Quaternary faulting of the northern Basin and Range province, Montana and Idaho. *Bull. seism. Soc. Am.* **77**, 1602–1625.

Susong, D. D., Janecke, S. U. & Bruhn, R. L. 1990. Structure of a fault segment boundary in the Lost River fault zone, Idaho, and possible effect on the 1983 Borah Peak earthquake rupture. *Bull. seism. Soc. Am.* **80**, 57–68.

Vincent, K. R. 1985. Measurement of vertical tectonic offset using longitudinal profiles of faulted geomorphic surfaces near Borah Peak, Idaho—A preliminary report. In: *Proc. Workshop XXVIII on the Borah Peak, Idaho, Earthquake* (edited by Stein, R. S. & Bucknam, R. C.). *U.S. geol. Surv. Open-file Rep.* **85-290**, 76–96.

Wallace, R. E. 1970. Earthquake recurrence intervals on the San Andreas fault. *Bull. geol. Soc. Am.* **81**, 2875–2890.

Wallace, R. E. 1977. Profiles and ages of young fault scarps, north-central Nevada. *Bull. geol. Soc. Am.* **88**, 1267–1281.

Wallace, R. E. 1984. Fault scarps formed during the earthquakes of October 2, 1915, in Pleasant Valley, Nevada, and some tectonic implications. *Prof. Pap. U.S. geol. Surv.* **1274-A**.

Ward, S. N. & Valensise, G. R. 1989. Fault parameters and slip distribution of the 1915 Avezzano, Italy, earthquake derived from geodetic observations. *Bull. seism. Soc. Am.* **79**, 690–710.

Wheeler, R. L. 1987. Boundaries between segments of normal faults—Criteria for recognition and interpretation. In: *Proc. Conference XXXIX—Directions in Paleoseismology* (edited by Crone, A. J., & Omdahl, E. M.). *U.S. geol. Surv. Open-file Rep.* **87-673**, 385–398.

Wheeler, R. L. 1989. Persistent segment boundaries on Basin-Range normal faults. In: *Proc. of Workshop XLV—Fault Segmentation and Controls of Rupture Initiation and Termination* (edited by Schwartz, D. P. & Sibson, R. H.). *U.S. geol. Surv. Open-file Rep.* **89-315**, 432–444.

Wheeler, R. L. & Krystinik, K. B. 1987. Persistent and nonpersistent segmentation of the Wasatch fault zone, Utah—Statistical analysis for evaluation of seismic hazard. In: *Assessment of Regional Earthquake Hazards and Risk along the Wasatch Front, Utah* (edited by Gori, P. L. & Hays, W. W.). *U.S. geol. Surv. Open-file Rep.* **87-585**, B1–B124.

Wyss, M. 1979. Estimating maximum expectable magnitude of earthquakes from fault dimensions. *Geology* **7**, 336–340.

Zhang, P., Slemmons, D. B. & Mao, F. 1991. Geometric pattern, rupture termination and fault segmentation of the Dixie Valley–Pleasant Valley active normal fault system, Nevada, U.S.A. *J. Struct. Geol.* **13**, 165–176.

Zoback, M. L. 1983. Structure and Cenozoic tectonism along the Wasatch fault zone, Utah. In: *Tectonic and Stratigraphic Studies in the Eastern Great Basin* (edited by Miller, D. M., Todd, V. R. & Howard, H. A.). *Mem. geol. Soc. Am.* **157**, 3–27.